

Microfabricated atomic clocks and magnetometers

S Knappe^{1,2}, P D D Schwindt¹, V Gerginov^{1,3}, V Shah^{1,2}, L Liew⁴,
J Moreland⁴, H G Robinson¹, L Hollberg¹ and J Kitching¹

¹ Time and Frequency Division, National Institute of Standards and Technology, Boulder, CO 80305, USA

² Department of Physics, University of Colorado, Boulder, CO 80309, USA

³ Department of Physics, University of Notre Dame, Notre Dame, IN 46556, USA

⁴ Electromagnetics Division, National Institute of Standards and Technology, Boulder, CO 80305, USA

E-mail: knappe@boulder.nist.gov

Received 30 September 2005, accepted for publication 9 December 2005

Published 31 May 2006

Online at stacks.iop.org/JOptA/8/S318

Abstract

We demonstrate the critical subsystems of a compact atomic clock based on a microfabricated physics package. The clock components have a total volume below 10 cm³, a fractional frequency instability of $6 \times 10^{-10}/\tau^{1/2}$, and consume 200 mW of power. The physics package is easily adapted to function as a magnetometer with sensitivity below 50 pT Hz^{-1/2} at 10 Hz.

Keywords: atomic clocks, atomic magnetometers, high-resolution spectroscopy, micro-optics

(Some figures in this article are in colour only in the electronic version)

1. Introduction

While the long-term precision of atomic clocks [1] is unsurpassed, the size and power required to run these devices has prevented their use in a variety of areas, particularly in applications that require portability or battery operation. These applications could include commercial communication systems [2], such as modern cellular telephone networks, as well as military navigation GNSS devices (Global Navigation Satellites Systems) [3–5]. The state of the art in compact commercial atomic frequency references are rubidium vapour cell devices with volumes near 100 cm³ that operate on a few watts of power and cost about \$1000.⁵

Miniaturization based on microelectromechanical systems (MEMS) offers many of the same compelling advantages to atomic frequency references as it does to other large-scale technologies. In addition to small size, a corresponding improvement in the device power dissipation is gained because the heat lost to the environment via the device surface is

⁵ See for example Symmetricom X-72 Precision Rubidium Oscillator, Stanford Research Systems PRS10 Rubidium Frequency Standard, Accubeat AR-100B Rubidium Frequency Standard, Temex iSource+Low Cost HPFRS, Frequency Electronics FE-5658A. Reference is for technical clarity and does not imply endorsement by NIST.

smaller. MEMS also could enable high-volume, wafer-based production of atomic clocks, which would substantially reduce cost. Such improvements would make atomic clocks useful in a variety of advanced applications where precision quartz frequency references are now used.

Furthermore, precision spectroscopy of atomic vapours, when implemented into other MEMS-based devices such as magnetometers and gyroscopes, could have similar advantages: the combination of atomic precision in low-power miniature packages.

2. The microfabricated atomic clock

2.1. The clock physics package

For the last two decades, atomic frequency references have been progressed to smaller and smaller devices. Most designs are based on lamp-pumped vapour cells with direct microwave interrogation [6–9]. Several commercial products are available to date (see footnote 5) with volumes near 100 cm³. They have a stable output frequency to about 10^{-11} at an integration time of one second and consume several watts of power. Encouraging progress was also been made on miniaturized vapour cell frequency references pumped by diode lasers

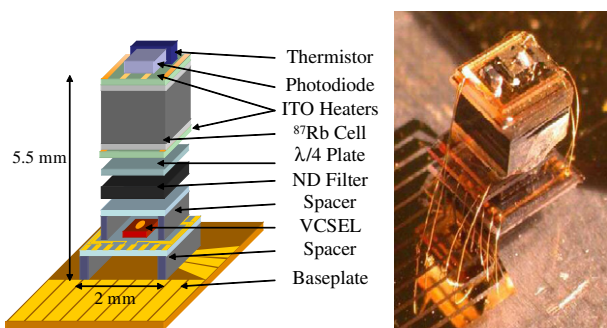


Figure 1. Schematic diagram (left) and photo (right) of a chip-scale atomic clock physics package.

rather than lamps [10] and on implementing other interrogation techniques such as coherent population trapping [11] for even smaller size and lower power consumption.

Recent work at NIST has focused on the development of the physics package [12], which contains the atoms that provide the fundamental reference frequency for the device. The physics package takes the gigahertz-range signal from a local oscillator (LO) as its input, compares the LO frequency to the resonant frequency of the atoms, and generates an output signal that depends on the frequency difference between the two. This output signal is then used to lock the oscillator frequency to the atoms.

The central part of the physics package [12] is an alkali vapour cell fabricated by use of MEMS techniques [13, 14]: a hole is etched through a silicon wafer using wet chemical etching (KOH) or deep reactive ion etching (DRIE) techniques. A borosilicate glass wafer is anodically bonded [15] onto each side of the silicon wafer to form a hermetically sealed cavity with two windows. Alkali atoms, along with an appropriate buffer gas, are sealed in the volume between the glass wafers. The cells are diced to cubes with volumes of roughly 5 mm^3 .

A laser beam is transmitted through the windows of the cell and is monitored with a photodiode. The light is provided by a vertical-cavity surface-emitting laser (VCSEL). It is shaped by a micro-optics assembly consisting of a polyimide spacer, two neutral density (ND) filters, and a quarter-wave plate before entering the cell. The cell is heated to $\sim 90^\circ\text{C}$ by two heaters made from a transparent indium tin oxide (ITO) film deposited onto a glass substrate and through which a current is passed; one heater is glued to each cell window. In order to tune the wavelength of the VCSEL to be resonant with the optical transition of the atoms, it is heated to $\sim 80^\circ\text{C}$ with a thin film resistor fabricated on the baseplate. The temperatures of the laser and the cell are monitored independently with chip thermistors. Wire bonds connect the VCSEL, cell heaters, thermistors, and photodiode to thin gold traces fabricated on the baseplate.

A photograph and schematic diagram of such a physics package are shown in figure 1. The VCSEL emits light at 795 nm, probing the D_1 line of the ^{87}Rb atoms contained in the vapour cell. The physics package has a total volume of $\sim 15 \text{ mm}^3$ and requires 110 mW of power at an ambient temperature of 25°C . It is surrounded by a $\sim 7 \text{ mm}$ long magnetic field coil and enclosed inside a magnetic shield of volume 0.7 cm^3 made from high-permeability metal.

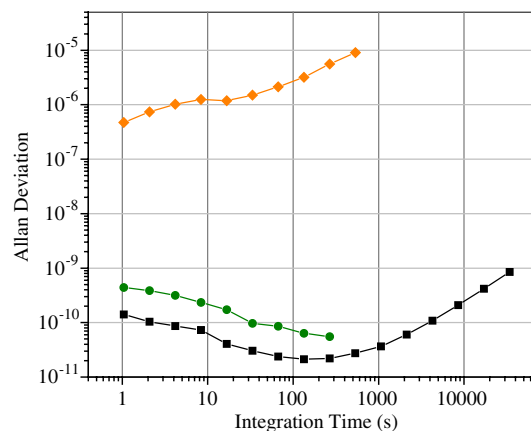


Figure 2. Fractional frequency instability measured for the chip-scale atomic clock components: the physics package shown in figure 1 (black squares), the free-running local oscillator (light grey diamonds), and the LO when locked to the atomic resonance using the physics package and small control electronics (grey dots).

The chip-scale clock uses coherent population trapping (CPT) [16, 17] to measure the frequency of the ground-state hyperfine splitting of ^{87}Rb atoms of roughly 6.8 GHz. This interrogation method allows precise probing of the very stable microwave frequency defined by the atoms without the need of a microwave cavity. In order to accomplish this, the VCSEL current (and thus its frequency) is modulated at 3.4 GHz, half the ground-state hyperfine frequency, and tuned such that the two first-order modulation sidebands are in resonance with the transitions from the two hyperfine-split ground states to a common excited state [18]. When the second harmonic of the modulation frequency at 6.8 GHz is exactly equal to the ground-state hyperfine splitting of the atoms, the transmission of the laser light through the cell increases. This transmission signal is then used to lock the local oscillator, which modulates the VCSEL current, to the atomic resonance. Under these conditions, a fractional frequency instability of 1.5×10^{-10} at one second of integration can be reached using the physics package described above (see black squares in figure 2).

It can be seen that frequency drifts are present at integration times longer than 100 s, which result from the fact that cell temperature and laser frequency were not stabilized in these measurements. Further characterization of the performance of the physics package and the vapour cells can be found in [19] and [20], where frequency stabilities of 6×10^{-12} at 1000 s of integration have been measured for similar vapour cells.

2.2. System assembly

The physics package was integrated with a LO operating at 3.4 GHz and miniature control electronics. The voltage-controlled oscillator is based on a coaxial resonator. Its phase noise is below -92 dBc at 10 kHz, it has a volume of roughly 0.15 cm^3 , and it consumes less than 5 mW of power [21]. Figure 2 shows the fractional frequency instability of the free-running local oscillator (light grey diamonds). A picture of the small local oscillator is shown in figure 3.

The control electronics subsystem is based on a phase-sensitive detector chip (AD630) that generates a dispersive

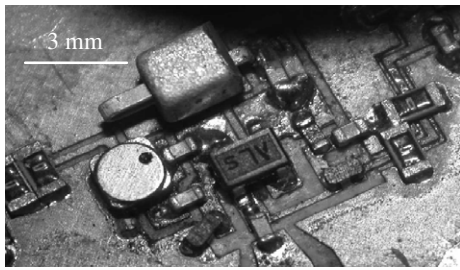


Figure 3. Picture of the miniature local oscillator.

error signal from the physics package output and locks the frequency of the local oscillator to the atomic resonance. This subsystem has a total volume of 6.3 cm^3 and requires 70 mW of power.

Together, the three frequency reference subsystems have a total volume of less than 10 cm^3 and require 200 mW of power to operate. A fractional frequency instability below $6 \times 10^{-10}/\tau^{1/2}$ is obtained (see grey dots in figure 2). Further miniaturization of the control electronics and lower power consumption of the physics package appears possible [22, 23]. We are planning in the near future to replace the analogue circuit with a digital circuit based on a microprocessor chip. Apart from the control of the LO frequency, three additional servo-loops will be implemented: one each to stabilize the temperature of the VCSEL and the vapour cell and one to lock the laser frequency to the atomic optical transition through feedback to the laser current. Furthermore, we are planning to implement better thermal isolation [23] to reduce the power consumption of the physics package and improve the frequency stability at integration times longer than 100 s . This could lead to chip-scale atomic frequency references of total volume 1 cm^3 and consuming less than 50 mW of power. This could enable CSACs to be used in battery-operated devices with applications that require microsecond timing out to a day. It could therefore bridge the gap between low-power temperature-compensated crystal oscillators (TCXOs), which cannot reach these stabilities, and small atomic clocks, which are too power hungry for many remote applications (see for example [4, 24]).

Finally, all individual parts of the physics package could be fabricated on individual wafers. The wafers would be stacked to assemble the packages and diced afterwards into individual physics packages. The use of MEMS fabrication techniques (figure 4) thus makes these devices appealing for commercialization.

3. The microfabricated atomic magnetometer

3.1. Introduction

Many applications, like magnetocardiography [25], underground and underwater ordinance detection [26], and geophysical mapping [27], rely on the measurement of magnetic fields with sensitivities around 1 pT . The magnetometers that meet these requirements often fill volumes of 100 cm^3 , dissipate a few watts of power and weigh several kilograms. Large-scale optical magnetometers [28] that use alkali metal vapours to measure the absolute magnetic field [29, 30] achieve

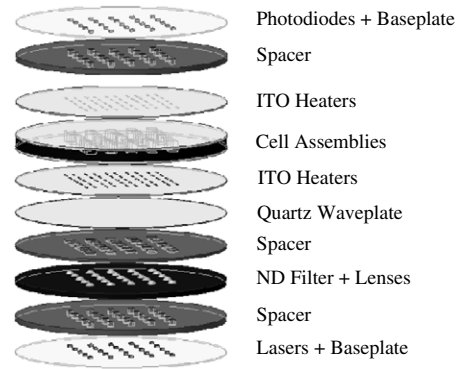


Figure 4. Wafer-level design for chip-scale atomic clock physics packages. All components are fabricated on individual wafers. The wafers are stacked to assemble the packages and diced afterwards into individual physics packages.

sensitivities of $\sim 1 \text{ fT Hz}^{-1/2}$, and rival superconducting quantum interference devices [31] in this regard without the need for cryogenic cooling. By miniaturizing an optical magnetometer on the basis of the coherent population trapping effect by a factor of 10^4 [32–34], we demonstrate a highly sensitive magnetic sensor that is millimetres in size, and has the potential to enable, for example, long-range remote sensing of magnetic fields on the basis of battery-operated disposable devices.

3.2. The magnetometer physics package

While the clock measures the frequency of two atomic ground states that are to first order independent of magnetic field, the magnetometer uses a very similar technique to measure the frequency splitting of two atomic ground states, which depends strongly on the magnetic field at the position of the atoms, i.e., the vapour cell. It is therefore possible to determine the total magnetic field at the location of the atoms by comparing the energy difference of magnetically sensitive states to the energy difference of magnetically insensitive states. A magnetometer of this type has been implemented at NIST [35] with a microfabricated structure shown in figure 1, based on the D_1 line of ^{87}Rb atoms. The active volume of the magnetic sensor is 1 mm^3 . With this physics package, magnetic fields can be measured with a sensitivity of $50 \text{ pT Hz}^{-1/2}$ over the frequency range of $10\text{--}100 \text{ Hz}$ (see figure 5). While this sensitivity is comparable to those of small and cheap magnetoresistive sensors (see for example [36]), it is the first demonstration of a chip-scale magnetometer based on an MEMS atomic vapour cell. Atomic magnetometers have the potential to reach sensitivities below 1 pT in sensitive volumes of 1 mm^3 (shot-noise limited fundamental sensitivity limit: $1 \text{ fT cm}^{3/2} \text{ Hz}^{-1/2}$ and even below, when spin-exchange suppressed [30]). Table top experiments have demonstrated magnetic sensitivities below $1 \text{ fT Hz}^{-1/2}$ in a sensitive volume of 0.3 cm^3 [30]. The fabrication methods presented in this paper could therefore enable the fabrication of small and inexpensive atomic magnetometers with sensitivities below $1 \text{ pT Hz}^{-1/2}$.

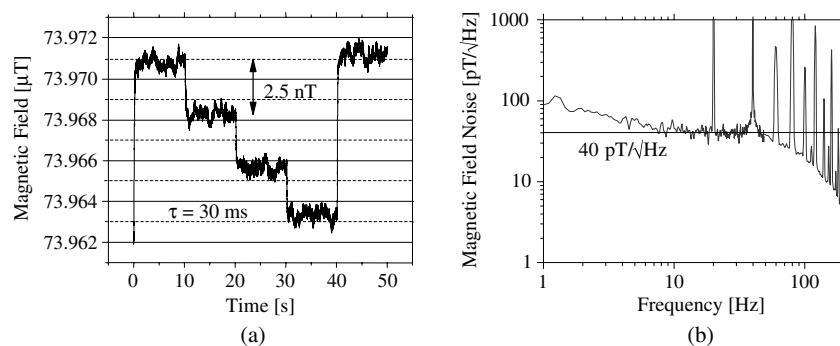


Figure 5. (a) The magnetometer signal plotted as a function of time as the magnetic flux is stepped in 10 s intervals. (b) Power spectral density of the magnetometer signal converted to units of magnetic flux density [35].

4. Conclusion

We have developed microfabricated atomic clocks and magnetometers based on rubidium vapour cells. The use of MEMS fabrication techniques allows the miniaturization of such atomic sensors. In addition to small size, a corresponding improvement in the device power dissipation is gained because the heat lost to the environment via the device surface is reduced. MEMS could also enable high-volume, wafer-based production of atomic clocks, which would substantially reduce cost.

Here, we demonstrate the three critical subsystems of a miniaturized atomic clock: the physics package, which performs the atomic spectroscopy, the local oscillator, which produces the clock signal, and the control electronics, which stabilize the LO frequency to the atomic resonance. Altogether, the clock subsystems have a volume below 5 cm^3 , and a fractional frequency instability of $6 \times 10^{-10} / \tau^{1/2}$, and consume under 200 mW of power.

We also demonstrate that this technology can be useful for implementing other atomic sensors, such as a microfabricated scalar magnetometer.

Acknowledgments

The authors thank Z Popović and A Brannon for the development and fabrication of the voltage-controlled oscillator.

This work was supported by NIST and the Microsystems Technology Office of the Defense Advanced Research Projects Agency (DARPA). This work is a contribution of NIST, an agency of the US government, and is not subject to copyright. Much of this work has been published in [12–14, 19–21, 23, 25].

References

- [1] Williams J H 2005 *Fifty Years of Atomic Time-Keeping: 1955 to 2005* vol 42, ed J H Williams (Bristol, UK: BIPM and IOP Publishing Ltd) (Special issue)
- [2] Kusters J A and Adams C A 1999 Performance requirements of communication base station time standards *RF Design* **22** 28–38
- [3] Fruehoff H 2001 Fast ‘direct-P(Y)’ GPS signal acquisition using a special portable clock *Proc. 33rd Ann. Precise Time and Time Interval (PTTI) Meeting* (Long Beach: US Naval Observatory) pp 359–69
- [4] Vig J R 1993 Military applications of high accuracy frequency standards and clocks *IEEE Trans. Ultrason. Ferroelectr. Freq. Control* **40** 522–7
- [5] Murphy J and Skidmore T 1994 A low-cost atomic clock: impact on the national airspace and GNSS availability *Proc. ION GPS-94; 7th Int. Meeting of the Satellite Division of the Institute of Navigation* (Salt Lake City, UT: ION)
- [6] Bloch M, Pasaru I, Stone C and McClelland T 1993 Subminiature rubidium frequency standard for commercial applications *Proc. IEEE Int. Frequency Control Symp.* (Salt Lake City, UT: IEEE) pp 164–77
- [7] McClelland T, Pasaru I, Shterman I, Stone C, Szekely C, Zacharski J and Bhaskar N D 1996 Subminiature rubidium frequency standard: performance improvements *Proc. IEEE Int. Frequency Control Symp.* (Honolulu, HI: IEEE) pp 1011–6
- [8] Rochat P, Leuenberger B and Stehlin X 2002 A new synchronized ultra miniature rubidium oscillator *Proc. IEEE Int. Frequency Control Symp.* (New Orleans, LA: IEEE) pp 451–4
- [9] Koyama Y, Matsura H, Atsumi K, Nakamuta K, Sakai M and Maruyama I 2000 An ultra-miniature rubidium frequency standard *Proc. IEEE Int. Frequency Control Symp.* (Kansas City, MO: IEEE) pp 694–99
- [10] Liberman I and Chantry P J 1997 Miniature atomic frequency standard *US Patent Specification* 5,670,914
- [11] Vanier J, Levine M, Kendig S, Janssen D, Everson C and Delany M 2004 Practical realization of a passive coherent population trapping frequency standard *Proc. IEEE Int. Frequency Control Symp.* (Montreal, PQ: IEEE) pp 92–9
- [12] Knappe S, Shah V, Schwindt P D D, Hollberg L, Kitching J, Liew L A and Moreland J 2004 A microfabricated atomic clock *Appl. Phys. Lett.* **85** 1460–2
- [13] Liew L A, Knappe S, Moreland J, Robinson H, Hollberg L and Kitching J 2004 Microfabricated alkali atom vapor cells *Appl. Phys. Lett.* **84** 2694–6
- [14] Knappe S, Velichansky V L, Robinson H G, Liew L, Moreland J, Kitching J and Hollberg L 2003 Atomic vapor cells for miniature frequency references *Proc. IEEE Int. Frequency Control Symp. and 17th European Frequency and Time Forum* (Tampa, FL: IEEE) pp 31–3
- [15] Wallis G and Pomerantz D 1969 Field assisted glass–metal sealing *J. Appl. Phys.* **40** 3946–9
- [16] Alzetta G, Gozzini A, Moi L and Orriols G 1976 Experimental-method for observation of Rf transitions and laser beat resonances in oriented na vapor *Nuovo Cimento B* **36** 5–20
- [17] Arimondo E 1996 Coherent population trapping in laser spectroscopy *Progress in Optics* vol 35, ed E Wolf (Amsterdam: Elsevier) pp 257–354

- [18] Vanier J, Godone A and Levi F 1998 Coherent population trapping in cesium: dark lines and coherent microwave emission *Phys. Rev. A* **58** 2345–58
- [19] Gerginov V, Knappe S, Schwindt P, Shah V, Hollberg L W and Kitching J 2005 Long-term frequency instability of CPT clocks with microfabricated vapor cells *J. Opt. Soc. Am. B* at press
- [20] Knappe S, Gerginov V, Schwindt P, Shah V, Robinson H G, Hollberg L and Kitching J 2005 Atomic vapor cells for chip-scale atomic clocks with improved long-term frequency stability *Opt. Lett.* **30** 2351–3
- [21] Brannon A, Breitbarth J and Popovic Z 2005 A low-power, low phase noise local oscillator for chip-scale atomic clocks *IEEE Microw. Theory Tech. Symp.* at press
- [22] Lutwak R, Deng J, Riley W, Varghese M, Leblanc J, Tepolt G, Mescher M, Serkland D K, Geib K M and Peake G M 2004 The chip-scale atomic clock-low-power physics package *36th Annual Precise Time and Time Interval (PTTI) Meeting* (Washington, DC: US Naval Observatory) pp 339–54
- [23] Kitching J, Knappe S, Schwindt P D D, Shah V, Hollberg L, Liew L and Moreland J 2004 Power dissipation in a vertically integrated chip-scale atomic clock *IEEE Int. Frequency Control Symp.* (Montreal, PQ: IEEE) pp 781–4
- [24] Vig J R 1992 Introduction to quartz frequency standards *Technical Report SLCET-TR-92-1* Army Research Laboratory, Electronics and Power Sources Directorate Available at <http://www.ieee-uffc.org/freqcontrol/quartz/vig/vigtoc.htm>
- [25] Bison G, Wynands R and Weis A 2005 Optimization and performance of an optical cardiomagnetometer *J. Opt. Soc. Am. B* **22** 77–87
- [26] Clem T R 1998 Superconducting magnetic gradiometers for underwater target detection *J. Naval Eng.* **110** 139–49
- [27] Sarma B S P, Verma B K and Satyanarayana S V 1999 Magnetic mapping of Majhgawan diamond pipe of central India *Geophysics* **64** 1735–9
- [28] Dehmelt H 1957 Modulation of a light beam by precessing absorbing atoms *Phys. Rev.* **105** 1924–5
- [29] Budker D, Kimball D F, Rochester S M, Yashchuk V V and Zolotarev M 2000 Sensitive magnetometry based on nonlinear magneto-optical rotation *Phys. Rev. A* **62** 043403
- [30] Kominis I K, Kornack T W, Allred J C and Romalis M V 2003 A subfemtotesla multichannel atomic magnetometer *Nature* **422** 596–9
- [31] Weinstock H 1996 SQUID sensors: fundamentals, fabrication, and applications *Book SQUID Sensors: Fundamentals, Fabrication, and Applications* (Dordrecht: Kluwer–Academic)
- [32] Nagel A, Graf L, Naumov A, Mariotti E, Biancalana V, Meschede D and Wynands R 1998 Experimental realization of coherent dark-state magnetometers *Europhys. Lett.* **44** 31–6
- [33] Stahler M, Knappe S, Affolderbach C, Kemp W and Wynands R 2001 Picotesla magnetometry with coherent dark states *Europhys. Lett.* **54** 323–8
- [34] Scully M O and Fleischhauer M 1992 High-sensitivity magnetometer based on index-enhanced media *Phys. Rev. Lett.* **69** 1360–3
- [35] Schwindt P D D, Knappe S, Shah V, Hollberg L, Kitching J, Liew L A and Moreland J 2004 Chip-scale atomic magnetometer *Appl. Phys. Lett.* **85** 6409–11
- [36] Robbes D, Dolabdjian C and Monfort Y 2002 Performances and place of magnetometers based on amorphous wires compared to conventional magnetometers *J. Magn. Magn. Mater.* **29** 393–7